Binary Neutron Star Mergers: Theory vs Observations

PHYS 815

Queen's University

Melissa Munoz
November 27, 2017

Contents

1 Historical introduction

In 1916, Einstein was first to propose the existence of gravitational radiation. During this time, the theoretical framework of compact astrophysical objects was developing. Notable contributions include the work of Schwarzschild (1916) and Kerr (1963) on black holes and rotating black holes respectively. Merging compact binary systems composed of neutron stars (NSs) or black holes (BHs) have since then been expected to be a dominant source of gravitational waves. Only recently, a century after its conception, have the first signals of gravitational radiation being observationally detected.

Double black hole systems (BH-BH) are expected to produce strong gravitational waves (GW). However, only double neutron star systems (NS-NS) or neutron black hole systems (NS-BH) systems are expected to produce coincident electromagnetic (EM) counterparts as well. The detection of EM signals in association to GW events can provide useful insight on the identification and localization of GW sources. Binary neutron star systems (i.e. NS-BH or NS-NS) systems are thus invaluable for the improvement of GW detections.

In section 2, we will briefly describe the evolution and fate that is expected of a binary neutron star system. Then, in section 3, we will discuss the joint theoretical framework behind GW sources and their EM counterparts that numerical simulations attempt to encode. Finally, in section 4, we will compare numerical predictions with observational evidence of GWs, namely, the recent LIGO observations.

2 Evolution and fate of binary neutron stars

It is generally well accepted that double compact binary systems are descendants of massive binary systems that survive and remain bound after two core collapse supernova explosions (Belczynski et al., 2008). Alternatively, it was been proposed that perhaps such compact systems can be formed via dynamical captures in dense globular clusters (Sadowski et al., 2008). Regardless of their predecessors, once a gravitationally bound compact object pair is formed, the merger process of such a system can be broadly described in three phases: the inspiral, merger and ringdown phase (Faber & Rasio, 2012) [See figure 1 for a cartoon illustration of the merger process and phases].

Inspiral

According to general relativity (GR), double compact binary systems are expected to emit gravitational radiation (e.g. Postnov & Yungelson, 2014). As a result, angular momentum is continuously lost and the binary components spiral-in. Peters & Mathews (1963) were first to derive the rate of orbital decay (predicted by Post-Newtonian mechanics). Consequently, the merger timescale due to GW emission is given by:

$$\tau_{\rm GW} = \frac{a}{|\dot{a}|} = \frac{5}{256}\frac{c^5}{G}\frac{a^4}{M^2\mu}\frac{(1-e^2)^{7/2}}{\left[1+\frac{73}{24}e^2+\frac{37}{96}e^4\right]}, \tag{1}$$

where c is the speed of light, G is the Gravitational constant, a is the orbital separation, $M = M_1 + M_2$ is the total mass, $\mu = {}^{M_1 M_2}/_{M_1 + M2}$ is the reduced mass and M_i are the masses

of the individual binary components. For a NS-NS system at an initial separation of 45 km, $\tau_{GW} \sim 10^8$ yr. As this is comfortably less than a Hubble time (i.e. 10^{10} yr), NS-NS mergers are therefore expected to occur (e.g. Rosswog & Brüggen, 2011). Similar conclusions can be derived for other variants of compact binary systems.

Merger

As a gravitationally bound system spirals in, tidal forces become increasingly more important. When the orbital separation is in the order of the stellar radii of the individual stars, the binary system becomes unstable and the merger process begins. (Davies et al., 1994) was first to conduct NS-NS merger simulations using 3D hydrodynamics. The developed work of Rosswog (2005) included BH-NS mergers and yielded the following conclusions. If both components are of similar masses (e.g. NS-NS mergers), the merger process is reminiscent of an inelastic collision, but in corotation. Spiral arms start to form and get wrapped around the central object in a ring like structure. However, if one component is significantly more massive than the other (e.g. BH-NS mergers), the lower mass star becomes tidally disrupted while it plunges. A large fraction of the less massive star's mass is essentially accreted onto the more massive star, while the remaining material is dynamically expelled. The typical timescale of the merger phase itself is in the order of a few milliseconds (Faber & Rasio, 2012).

Ringdown

The dynamical stabilization of the merger remnant is known as the ringdown phase. The final outcome of this merger process requires full general relativistic hydrodynamics and possibly even magnetohydrodynamics. For the coalescence of a NS-NS system, the merger product will lay in one of the following case: a BH, stable NS or unstable NS. This is difficult to constrain numerically as the hydrodynamics is highly sensitive to the choice of equation of state (EOS) used to describe the stellar interior (generally assumed to be a combination of piecewise polytropic models). According to the numerical work by Hotokezaka et al. (2011), both unstable NSs and apparently stable NSs are simply variants of short- or long-lived hypermassive neutrons stars (HMNSs). HMNSs are NSs with masses above the Chandrasekhar mass but below a certain critical mass above which, promptly after the merger, a black hole would be formed instead. Since the longevity of long-lived HMNSs is uncertain (defined to outlast at least 5 ms), they may indefinitely appear to be stable NS. In either case, both short- and long-lived HMNS will inevitably decay into a BH.

3 Theoretical predictions

3.1 Gravitational wave signal

In GR, gravitational radiation is a form of radiant energy that is treated as a wave, similar to how electromagnetic radiation is treated like a transverse wave in EM. Furthermore, GWs propagate at the speed of light and its energy is transported via the hypothetical particle, the graviton. Again, this is analogous to how photons carry the energy of EM waves at the speed of light.

A gravitational wave is characterized by the temporal evolution of its amplitude. The amplitude, h, of a GW is a dimensionless quantity that is related to the displacement of a test particle caused by the presence of a GW that perturbs the spacetime metric (e.g. ripples in the curvature of spacetime). Sophisticated numerical simulations use general relativistic hydrodynamics to predict the waveforms of emitting binary compact systems. As this is beyond the scope of this paper, we will suffice with an order-of-magnitude estimate.

In the general case of an object of mass, M, and radius, R, the amplitude of it's waveform will be given by

$$h \sim \frac{GM}{c^2}\frac{1}{r}\left(\frac{v}{c}\right)^2 = \frac{r_{\rm sch}}{r}\left(\frac{v}{c}\right)^2 \tag{2}$$

where $r_{\rm sch} = GM/c^2$ is the Schwarschild radius, v is the velocity of the object and r is its distance. Furthermore, the luminosity of such a GW event will be given by,

$$L_{\rm GW} \sim \frac{GM^2c}{R^2}\left(\frac{v}{c}\right)^6 = L_0\left(\frac{r_{\rm sch}}{R}\right)^2\left(\frac{v}{c}\right)^6, \tag{3}$$

where

$$L_0 \equiv \frac{c^5}{G} = 3.6 \times 10^{59}{\rm erg\,s^{-1}}. \tag{4}$$

These scaling relations can be derived from first principles in the context of GR (e.g. Shapiro & Teukolsky, 1986). We notice from eq.(1) that the amplitude falls off with distance (i.e. $1/r$ relationship) rendering distant signals difficult to detect. In addition, we can see that h and L_{WG} are maximal when R approaches $r_{\rm sch}$ and v approaches c. This is why merging compact binary systems were recognized to be primary sources of GWs: the radii of the binary components are in the order of their Schwarschild radius and their orbital velocities become increasingly relativistic prior to merging. This explains the amplitude spike and distinctive chirp in the waveform prior to the ringdown phase.

3.2 Electromagnetic counterpart

The inspiral and coalescence of binary compact objects are the most promising astrophysical sources of gravitational waves. If at least one component is a NS (i.e. BH-NS or NS-NS mergers), such systems are also expected to emit electromagnetic (EM) counterparts all across the EM spectrum, from energetic gamma-rays to low-frequency radio waves (Metzger et al., 2010). Figure 2 summarizes the expected EM counterparts and their characteristic timescales subsequent to a binary neutron star merger.

Simulating the expected EM counterparts from GW events is an important endeavor for observational comparisons. The EM counterparts are mainly powered by two sources: 1) the radioactive decay of r-process elements within the merger ejecta and 2) the accretion of merger ejecta onto the central compact object. The former process is related to the cataclysmic transient known as kilonovae, while the latter is related to short gamma-ray bursts.

The r-process and kilonovae

The r-process is a type of rapid neutron capture akin to the s-process or slow neutron capture process. Both of these two processes involve sequences of neutron captures:

$${}^{A}_{Z}X + n \rightarrow {}^{A+1}_{Z}X \tag{5}$$

and beta decays:

$$^{A+1}_{Z}X \rightarrow {}^{A+1}_{Z+1}X + e^- + \bar{\nu_e} \tag{6}$$

If the time between neutron captures is long compared to the timescale for beta decays, the process is said the be slow (s-process). On the other hand, if the time between neutron captures is short compared to the timescale for beta decays, the process is said to be rapid (r-process). Both s- and r-processes are capable of forging heavy elements past iron. However, considering the low Galactic heavy-element abundance, astrophysical sites that host such processes are likely to be rare.

The r-process is thought to predominantly occur in decompressing NS matter. NSs are incredibly dense and degenerate objects. They acquired their nuclear densities via successive electron captures:

$$p^+ + e^- \rightarrow n + \nu_e \tag{7}$$

This occurs during the core-collapse supernova phase prior to the NS formation. The free neutrons produced are naturally unstable and would therefore, under normal circumstances, revert back to protons via the beta decay

$$n \rightarrow p^+ + e^- + \bar{\nu_e} \tag{8}$$

However, the high degree of electron degeneracy in NSs inhibits this process. Instead, starting from iron, the free neutrons take part in a chain of neutron captures that is responsible for synthesizing neutron-rich nuclei (i.e. neutronization). If, at this phase, the medium is expanding, the decrease in density will lift the electron degeneracy which will in turn allow for beta-decays to occur within a soup of neutron-rich nuclei. First proposed by Lattimer & Schramm (1976) and further developed by Eichler et al. (1989), NS mergers became highly suspected to be a dominant source of r-process nucleosynthesis. Within a matter of seconds, the expanding ejecta triggers the r-process and a wide variety heavy r-process nuclei are forged (including gold and platinum). The r-process alone is capable of synthesizing more than half the heavy-elements part iron, consequently enriching the interstellar medium (ISM).

As the ejecta continuously expands and becomes translucent, radiation is rapidly released in the form of a kilonova. Kilonovae are cataclysmic transients of thermal radiation associated with the ejecta of binary NS mergers. Although Li & Paczyński (1998) were fist to present a crude model for kilonovae, the inclusion of r-process heating was only accomplished in (Metzger et al., 2010). Recent one dimensional Monte Carlo radiation transfer calculations by Metzger (2017) predict a characteristic peak luminosity timescale of

$$t_{\rm kn} \approx 1.6\,{\rm days} \times \left(\frac{M_{\rm ej}}{0.01 M_\odot}\right)^{1/2} \left(\frac{v_{\rm ej}}{0.1c}\right)^{-1/2} \left(\frac{\kappa_{\rm ej}}{1{\rm cm}^2{\rm g}^{-1}}\right)^{1/2}, \tag{9}$$

and a characteristic peak luminosity of

$$L_{\rm kn} \approx 5 \times 10^{40}\,{\rm erg\ s^{-1}} \times \left(\frac{M_{\rm ej}}{0.01 M_\odot}\right)^{1-\alpha/2} \left(\frac{v_{\rm ej}}{0.1c}\right)^{\alpha/2} \left(\frac{\kappa_{\rm ej}}{1{\rm cm}^2{\rm g}^{-1}}\right)^{-\alpha/2}. \tag{10}$$

where $M_{\rm ej}$, $v_{\rm ej}$ and $\kappa_{\rm ej}$ are the mass, velocity and opacity of the ejecta and $\alpha \sim 1/3$. The characteristics of kilonovae are therefore highly dependent on the merger ejecta. The merger

ejecta is generally composed of a disk wind ejecta and a tidal tail. The disk wind ejecta is essentially comprised of the circumburst material that accretes onto the central object. On the other hand, the tidal tail consists of the dynamically ejected material that escapes accretion. In NS-NS systems, the amount of dynamical ejecta ranges from $10^{-4} - 10^{-2}\ M_{\odot}$. Since NS-BH systems have stronger tidal interactions, they can have ejecta masses up to 0.1 $M_{\odot}$. In both cases, the ejecta material can obtain moderately relativistic velocities ranging from $0.1\,c$ to $0.3\,c$. With these values in mind, we can see from eqs.(9) and (10), that these events achieve a peak luminosity of $\sim 10^{41}$ erg s^{-1} within a few days. As this is a factor of 10^3 larger then novae, they were termed kilonovae by Metzger et al. (2010).

Equatorial regions of the ejecta are generally associated with higher opacities in the order of $\sim 100\text{cm}^2$. This will produce a lanthanide-rich (atomic masses A > 140) ejecta and transient that is of longer duration (order several days to a week), peaking in the infrared. This is referred to as a red kilonova. Conversely, polar regions of the ejecta are associated with lower opacities in the order of $\sim 1\text{cm}^2$. This will produce a lanthanide-poor ($90<$A<140) ejecta and a transient that is of shorter duration (order of days), peaking in the optical. This is referred to as a blue kilonova Metzger (2017). Depending on the viewing angle, manifestations of both blue and red kilonova are possible. The nature of the remnant object also influences the colour of the kilonova. For instance, if a prompt BH is formed after the merger, the ejecta is mainly neutron-rich which is will result in a red kilonova. If instead a HMNS is formed, the ejecta will be affected by neutrino emission that suppresses the r-process (via the week interaction). This will result in a blue kilonova. See figure 3 for sample blue and red kilonovae simulations across the optical band.

If is interesting to note that shocks between the ejecta and ISM can occur and produce significant radio emission. Unfortunately, the timescale for the radio emission is in the order of years and are thus difficult to detect in association with rapidly evolving transients Metzger & Berger (2012).

To summarize, a more massive ejecta will result in a brighter and longer-lasting kilonova. Conversely, a faster ejecta will also result in a brighter, but shorter-lived kilonova. Finally, a low-opacity ejecta will produce a blue kilonova, while a high-opacity ejecta will produce a red kilonova.

Accretion and short gamma-ray burts

Gamma-ray burst (GRBs) are extremely energetic yet brief transients. Indeed, GRBs are the most luminous astrophysical events across the electromagnetic spectrum. GRBs are divided in two subclasses based on their duration (Berger, 2014): long-duration gamma-ray bursts (long GRBs) have durations above 2 s, while short-duration gamma-ray burst (short GRBs), below 2 s.

The bimodality of GRBs suggests that two different triggering mechanisms are at play. Indeed, long GRBs are thought to be associated with core-collapse supernovae and can therefore be used as precursors. Even prior to the existence of kilonova, the work by Paczynski (1986) pointed out that short GRBs are of cosmological origin. This eventually lead to the general consensus that short GRBs are probably linked to merging binary neutron star systems. These theories are supported by a variety of observation evidences, such as their low incidence rate and spatial distribution. Most convincingly is the compactness problem. The

large amount of energy they release on such a short timescale can only be explained by a relativistic ejection of matter from a very small emitting region: a compact object. If short GRBs are indeed related to binary neutron stars mergers, they should largely contribute to the EM counterparts of GWs.

Short GRBs are identifiable by their quick prompt emission (order of milliseconds), succeeded with a slowly decaying afterglow (order of days). Powered by accretion, short GRBs emit powerful non-thermal radiation in the form of gamma-rays (Metzger & Berger, 2012). The prompt emission (or "fireball "), is attributed to the high-energy gamma-rays that originate from collimated relativistic jets. The jets are formed centrally above and below the circumburst accretion disk. The gamma-rays are expected to achieve their peak luminosities of $\sim 10^{51}$ erg s^{-1} within less than a second and are essentially immediately detectable after a GW event (Berger, 2014). However, a short GRB's gamma-rays can only be perceived observationally if the collimated jets are directed towards the observer (i.e. on axis short GRB). To make matters worse, due to relativistic beaming, the viewing angle becomes unfortunately narrower, which is observationally constrained in the range of $3 - 10°$.

Following the prompt emission, remains an afterglow. The afterglow is in fact created from the shock between the relativistic jet and the ISM. This can produce X-rays, but optical and radio emission as well. The X-ray afterglow emission is expected to last within 1-100 seconds. For an off-axis short GRB, a delayed onset of X-rays can occur. Such X-rays typically exceed luminosities of 10^{44} erg s^{-1}. The optical afterglow emission is expected to peak at a luminosity in the order of 10^{42} erg s^{-1} within a timescale of 1-10 days (Berger, 2014). As for the extended radio emission, little information is known about its peak luminosity as its peak time is poorly constrained and can range anywhere from months to years. Furthermore, optical and radio afterglows have the advantage of being observable regardless of the viewing angle. Since the interaction of the jets and the surrounding medium causes the material to decelerate, the emission will disperse into the line of sight of the observer. However, this comes with the compensation of a significantly reduced luminosity.

4 Observational Evidence

Advanced LIGO is a modified Michelson interferometer that is optimized for measuring the space time metric distortions due to GW, otherwise known as the strain. The LIGO observations provide a temporal evolution of the strain that can be fitted to numerical waveform calculations in order to obtain fundamental source properties, such as the individual sources masses. This is typically accomplished by first constraining the chirp mass, $\mathcal{M} = {(M_1 M_2)^{3/5}}/{(M_1 + M_2)^{-1/5}}$, and the total mass, $M = M_1 + M_2$. This is because the the waveform components (i.e. inspiral, merger and ringdown phases) have different sensitivities to the these two quantities. In fact, the waveform of the inspiral phase is primarily governed by the chirp mass. Meanwhile, the merger and ringdown phases are predominantly determined by the total mass. See table A, for a summary of previous LIGO detections.

On August 17, 2017, the Laser Interferometer Gravitational-Wave Observatory (LIGO) detected its 6th GW event: a NS-NS merger candidate. All previous detections were binary black hole mergers that provided strong direct evidence of GWs. However, the nature of this newest detection, GW170817, has the potential to finally unite kilonovae and short GRBs

to a common ancestor: binary neutron star mergers. Understanding the importance behind this GW event, GW170817 was hastily followed by numerous gamma-ray, X-ray and optical observations. The major contributions are listed in table A and illustrated in figure 5.

Gamma-ray detections at the location of GW170817 lead to the identification of a short GRB, GRB 170817A. Occurring shortly after a GW event, this provides strong evidence for the cosmological origin of short GRBs. Follow up spectroscopic observations spanning the ultraviolet and infrared region suggest the presence of a blue and red kilonova, thus constraining the viewing angle of the merger. The extensive amount of spectroscopic data obtained can also be used to probe the velocity distribution within the ejecta. In agreement with theory, moderately relativistic velocities of $\sim 0.1 - 0.3c$ were obtained (Abbott et al., 2017c). In addition, features of r-process nucleosynthesis elements were detected in the spectra. This is consistent with the idea that kilonova are powered by the r-process that can occur in decompressing NS ejecta. Finally, the detections of delayed X-ray and radio counterparts can be associated to a short GRB afterglow. Characterizing the spectral hardness (or softness) of X-ray sources can reveal useful insight on the geometry of the outflowing matter. In fact, hard X-rays were detected which is indicative of colliding winds Abbott et al. (2017d). Furthermore, an external radio source was detected in the region of GW170817 which was first mistaken for a genuine radio counterpart. Fortunately, the outlier radio source could be linked to the activity of NGC 4993's active galactic nucleus (AGN)! NGC 4933 has a known distance of ~ 40 Mpc. Remarkably, this value is consistent with the best-fitted distance $\sim 40^{+8}_{-14}$ that was obtained during the waveform fitting procedure.

In short, GW170817 was detected all across the electromagnetic spectrum, including gamma-rays, X-rays, optical bands and radio bands. As predicted by theory, they were respectively detected within seconds, hours, days and weeks after the merger event.

5 Conclusion

Double compact binary mergers are the perfect laboratories for hosting the production of gravitational waves. However, unique to binary neutron star mergers is the emission of electromagnetic counterparts that span all across the electromagnetic spectrum. Indeed, gamma-rays are expected to be emitted within a matter of milliseconds after a gravitational wave event, while radio emission could last up to years.

Though indirect evidence for gravitational waves have previously been implied (e.g. Hulse & Taylor, 1975), only recently has their existence been directly detected with long awaited solid observational evidence. In addition, the latest LIGO detection of a coalescing NS-NS candidate almost flawlessly unites theoretical predictions with observations all across the electromagnetic spectrum.

While the implications are numerous, they were not thoroughly discussed. For instance, observational constrains for compact binary merger rates can be estimated. This value is important for population synthesis calculations (e.g. Belczynski et al., 2008). Furthermore, the detection of GW events may also have a huge impact on cosmology as it could potentially constrain the Hubble parameter or even provide a mass limit on the hypothetical particle, the graviton (Abbott et al., 2017b).

References

Abbott, B. P., Abbott, R., Abbott, T. D., Acernese, F., Ackley, K., Adams, C., Adams, T., Addesso, P., Adhikari, R. X., Adya, V. B., & et al. 2017a, *Astrophys. J. Lett.*, 848, L13

—. 2017b, Physical Review Letters, 118, 221101

—. 2017c, Physical Review Letters, 119, 161101

—. 2017d, *Astrophys. J. Lett.*, 848, L12

Belczynski, K., Kalogera, V., Rasio, F. A., Taam, R. E., Zezas, A., Bulik, T., Maccarone, T. J., & Ivanova, N. 2008, *Astrophys. J. Suppl.* , 174, 223

Berger, E. 2014, *Ann. Rev. Astron. Astrophys.*, 52, 43

Davies, M. B., Benz, W., Piran, T., & Thielemann, F. K. 1994, *Astrophys. J.*, 431, 742

Eichler, D., Livio, M., Piran, T., & Schramm, D. N. 1989, *Nature*, 340, 126

Faber, J. A. & Rasio, F. A. 2012, Living Reviews in Relativity, 15, 8

Hotokezaka, K., Kyutoku, K., Okawa, H., Shibata, M., & Kiuchi, K. 2011, *Phys. Rev. D*, 83, 124008

Hulse, R. A. & Taylor, J. H. 1975, *Astrophys. J. Lett.*, 195, L51

Lattimer, J. M. & Schramm, D. N. 1976, *Astrophys. J.*, 210, 549

Li, L.-X. & Paczyński, B. 1998, *Astrophys. J. Lett.*, 507, L59

Metzger, B. D. 2017, Living Reviews in Relativity, 20, 3

Metzger, B. D. & Berger, E. 2012, *Astrophys. J.*, 746, 48

Metzger, B. D., Martínez-Pinedo, G., Darbha, S., Quataert, E., Arcones, A., Kasen, D., Thomas, R., Nugent, P., Panov, I. V., & Zinner, N. T. 2010, *Mon. Not. Roy. Astron. Soc.*, 406, 2650

Paczynski, B. 1986, *Astrophys. J. Lett.*, 308, L43

Peters, P. C. & Mathews, J. 1963, Phys. Rev., 131, 435

Postnov, K. A. & Yungelson, L. R. 2014, Living Reviews in Relativity, 17, 3

Rosswog, S. 2005, *Astrophys. J.*, 634, 1202

Rosswog, S. & Brüggen, M. 2011, Introduction to High-Energy Astrophysics

Sadowski, A., Belczynski, K., Bulik, T., Ivanova, N., Rasio, F. A., & O'Shaughnessy, R. 2008, *Astrophys. J.*, 676, 1162

Shapiro, S. L. & Teukolsky, S. A. 1986, Black Holes, White Dwarfs and Neutron Stars: The Physics of Compact Objects, 672

A Tables and figures

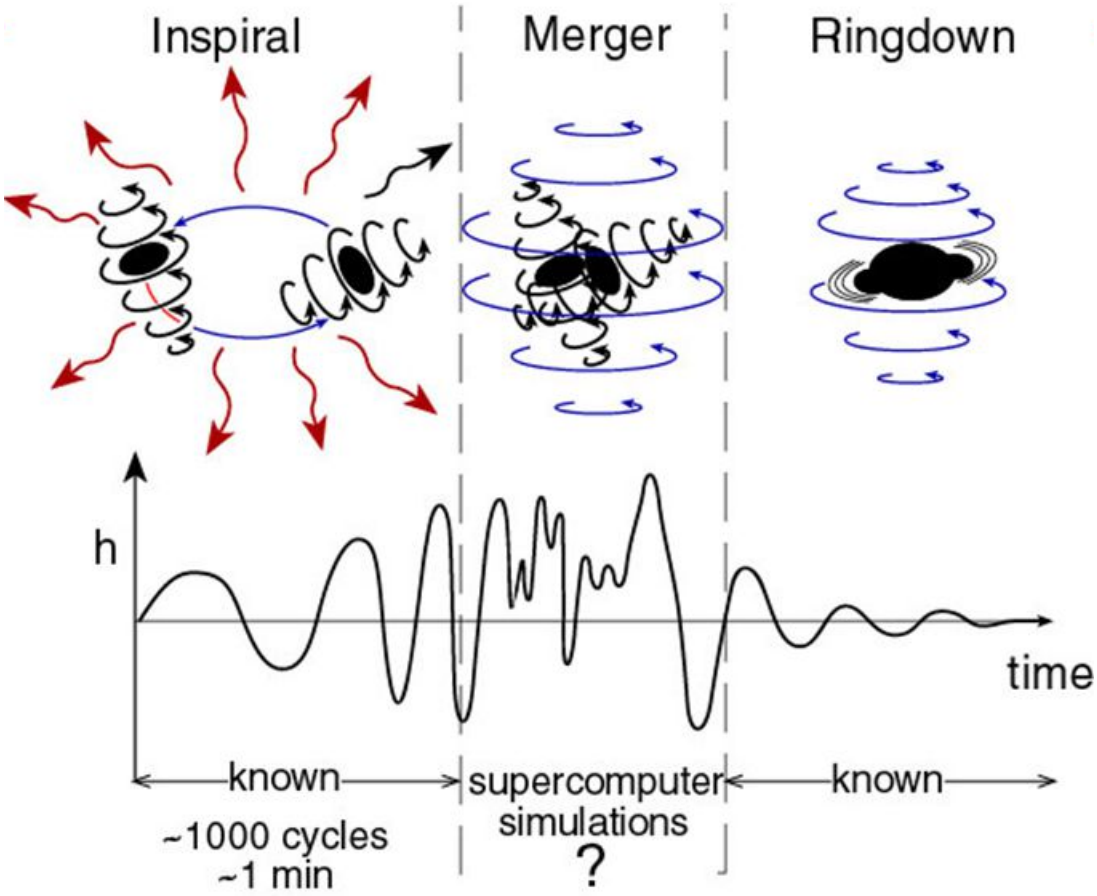

Figure 1: Cartoon illustrating the different merger phases of double compact objects. Adapted from Faber & Rasio (2012).

Table 1: Summary of LIGO's GW detections and source properties

	Merger system			Merger remnant		
GW event	Type	M_1 $[M_\odot]$	M_2 $[M_\odot]$	Type	M $[M_\odot]$	D [Mpc]
GW150914	BH-BH	$35.5^{+5.0}_{-3.4}$	$29.8^{+3.3}_{-4.3}$	BH	$62.2^{+3.7}_{-3.4}$	400^{+160}_{-180}
GW151226	BH-BH	$14.2^{+8.3}_{-3.7}$	$7.5^{+2.3}_{-2.3}$	BH	$20.8^{+6.1}_{-1.7}$	400^{+180}_{-190}
GW170104	BH-BH	$31.2^{+8.4}_{-3.4}$	$19.4^{+5.3}_{-5.9}$	BH	$48.7^{+5.7}_{-4.6}$	880^{+450}_{-390}
GW170608	BH-BH	12^{+7}_{-2}	7^{+2}_{-2}	BH	$18.0^{+4.8}_{-0.9}$	340^{+140}_{-140}
GW170814	BH-BH	$30.5^{5.7}_{-3.0}$	$25.3^{+2.8}_{-4.2}$	BH	$53.2^{+3.2}_{-2.5}$	540^{+130}_{-210}
GW170817	NS-NS	$1.36 - 1.60$	$1.17 - 1.36$	BH or NS	$2.7^{+0.05}_{-0.1}$	40^{+8}_{-14}

Table 2: Chronology of GW170817's follow up observations

Time post-merge	Detection	Observatory
~ 1.7 seconds	GRB 170817A: Weak gamma-ray counterpart	*Fermi* Gamma-ray Space Telescope
~ 11 hours	AT 2017gfo: Bright optical transient	Swope Telescope
~ 48 hours	Follow-up ultraviolet observations (faded)	Namely *Swift* and HST
~ 10 days	Follow-up optical and infrared observations (reddening)	Namely by DECam, Gemeni-South
~ 9 days	X-rays counterpart	*Chandra*
~ 16 days	Radio counterpart	VLA

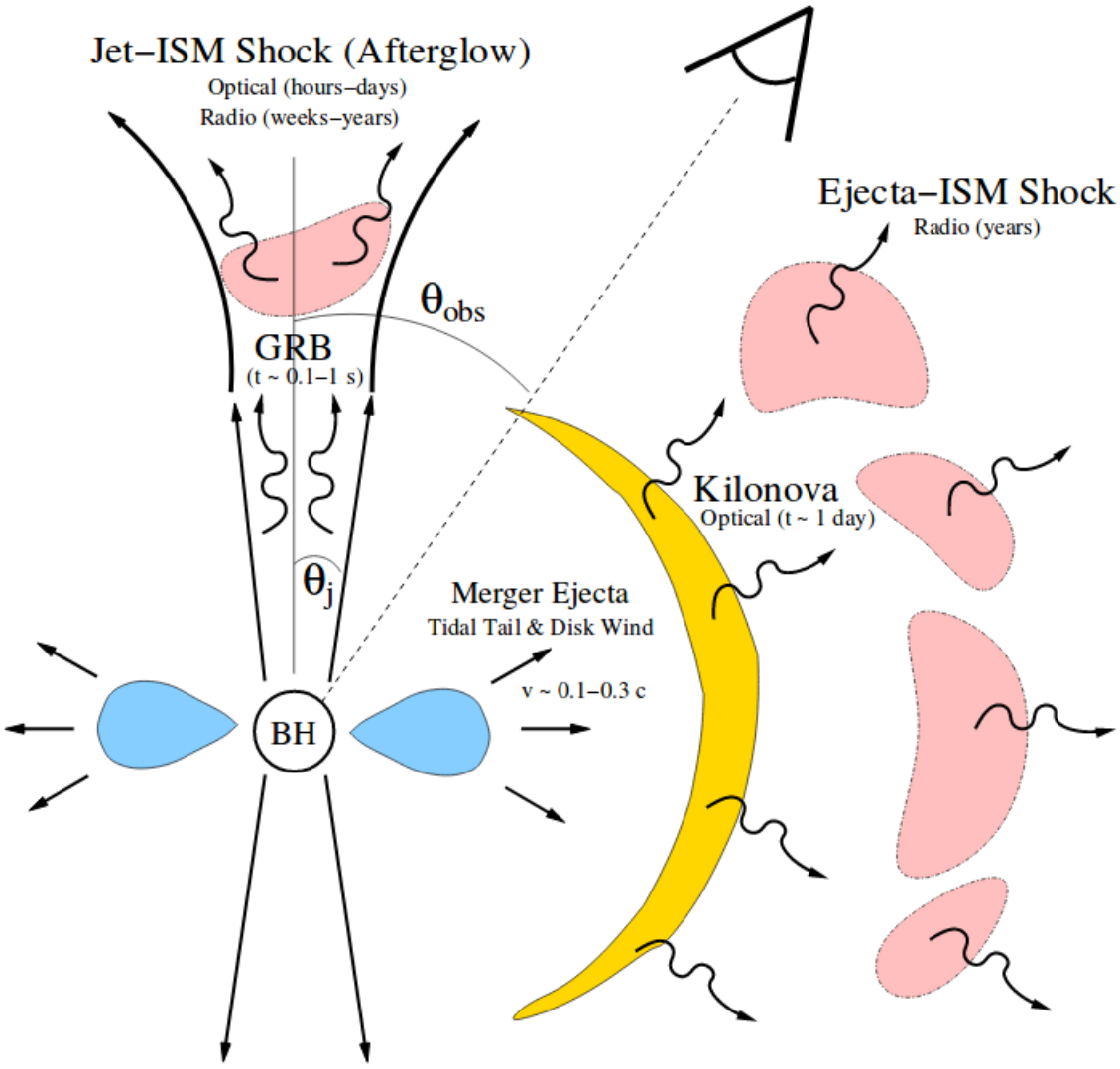

Figure 2: Cartoon illustrating the expected EM counterparts following a GW event. Adapted from Berger (2014).

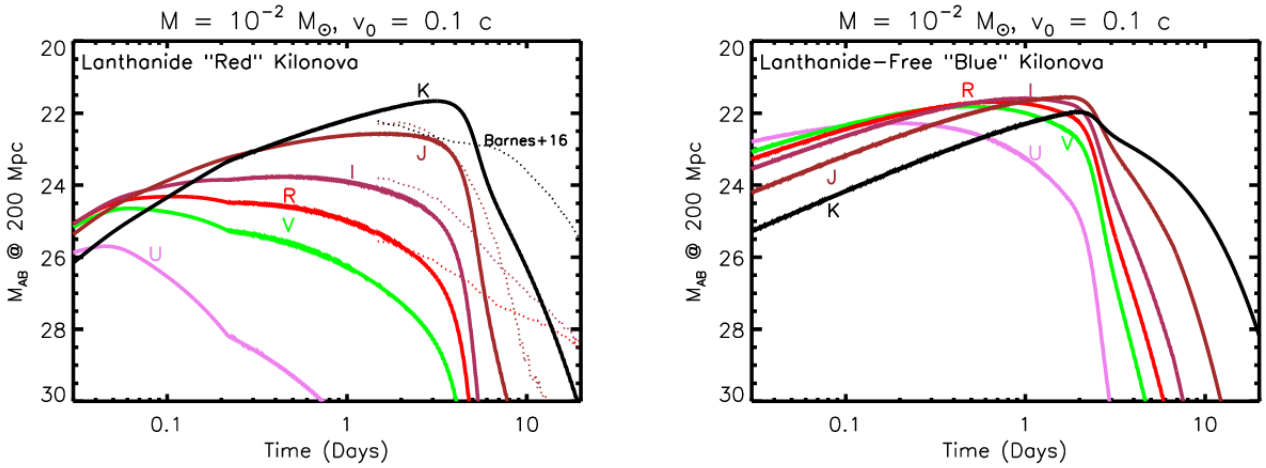

Figure 3: Sample numerical calculations of red and blue kilonovae. Adapted from Metzger (2017).

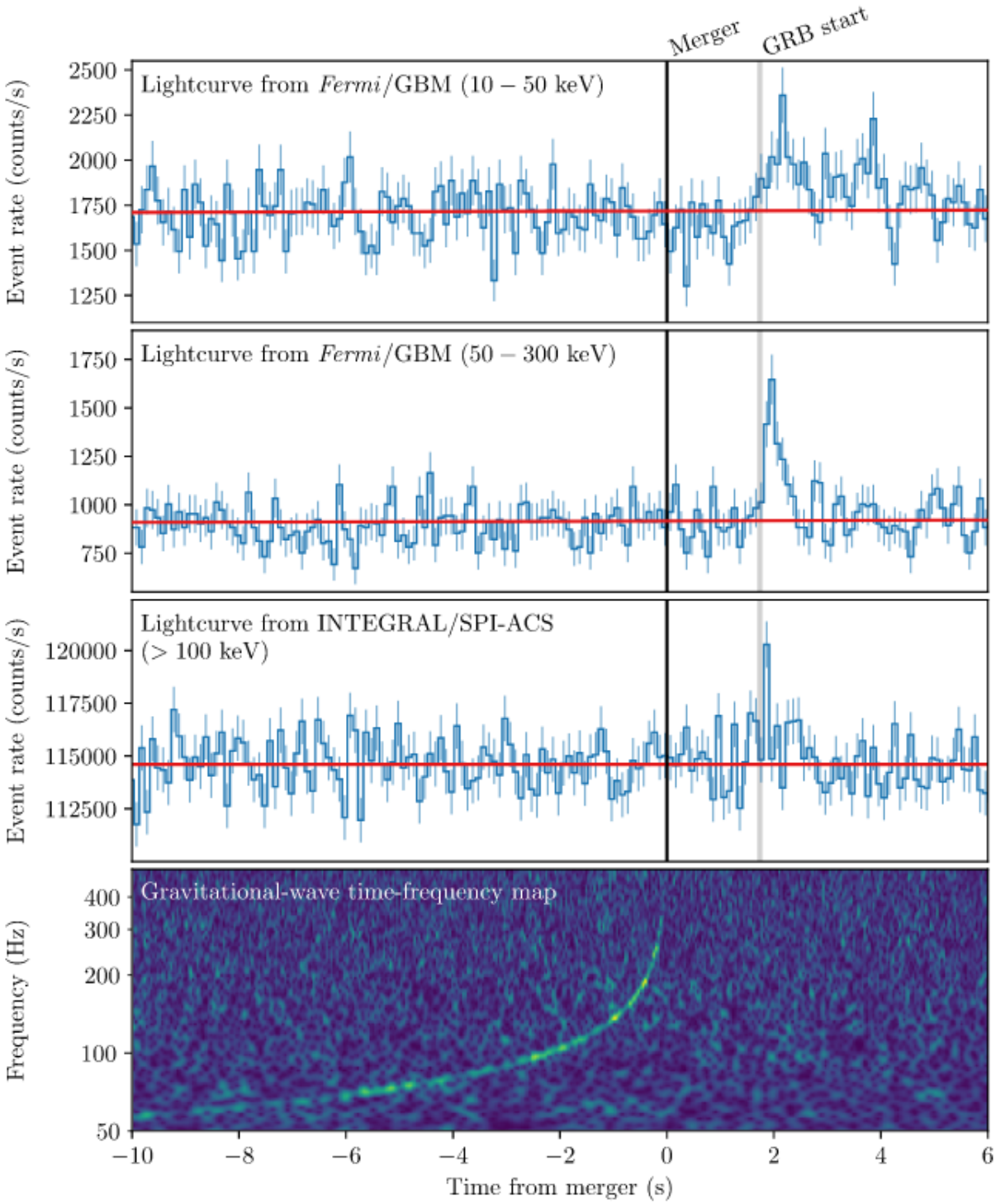

Figure 4: Newest LIGO detection: GW signal, GW170817, and coincident short GRB signal, GRB 170817A. Adapted from Abbott et al. (2017a).

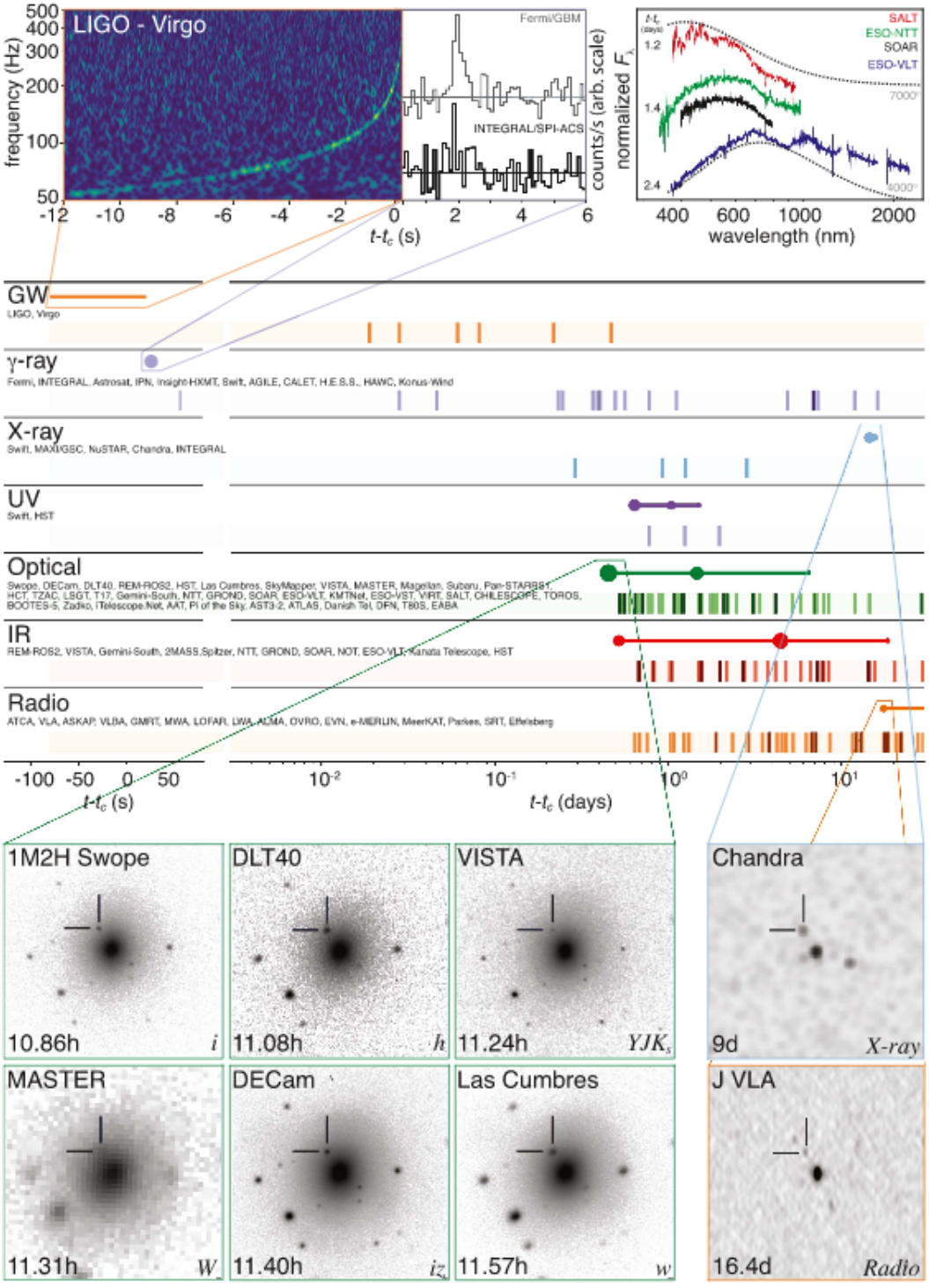

Figure 5: Follow up observations for GW170817. Adapted from Abbott et al. (2017d).